

***Electronic Supplementary Information (ESI)***

**Synthesis of Anion-Functionalized Mesoporous Poly(ionic liquid)s *via* a  
Microphase Separation-Hypercrosslinking Strategy: Highly Efficient Adsorbents  
for Bioactive Molecules**

Xian Suo, Ling Xia, Qiwei Yang, Zhiguo Zhang, Zongbi Bao, Qilong Ren, Yiwen Yang, Huabin Xing\*

Key Laboratory of Biomass Chemical Engineering of Ministry of Education,  
College of Chemical and Biological Engineering, Zhejiang University,  
Hangzhou 310027, China.

\*Corresponding author: Huabin Xing

E-mail: xinghb@zju.edu.cn

## Materials

All chemicals were used without further purification, unless otherwise noted. Divinylbenzene (DVB, 80%), 1-vinylimidazole (99%), ( $\pm$ )  $\alpha$ -tocopherol (analytical standard, 99.9%), (+)  $\gamma$ -tocopherol (analytical standard, 98%), (+)  $\delta$ -tocopherol (analytical standard, 95.2%) and Dowex Monosphere 550A UPW resin (OH type) were purchased from Sigma-Aldrich. Bromoethane (98%), acetic acid (>99%), and Amberlite XAD-4 resin were obtained from Alfa Aesar. Hexanoic acid (99%) was purchased from J&K Scientific Ltd. (China). Butyric acid (99%), octanoic acid (99%), decanoic acid (99%), lauric acid (98%), myristic acid (99%), palmitic acid (97%), 2,2'-azobis(2-methylpropionitrile) (AIBN, 99%, recrystallized), Amberlite 717 resin (AR), *p*-cresol (98%) and 2,6-dimethylphenol (99%), ( $\pm$ )- $\alpha$ -tocopherol (96%), and hydrochloric acid (HCl) standard solution (1 mol L<sup>-1</sup>) were obtained from Aladdin Reagent Co., Ltd. (China). 1-ethyl-3-vinylimidazolium tetrafluoroborate ([EVIM][BF<sub>4</sub>],  $\geq$ 99%), 1-ethyl-3-vinylimidazolium hexafluorophosphate ([EVIM][PF<sub>6</sub>],  $\geq$ 99%), and 1-ethyl-3-vinylimidazolium bis(trifluoromethylsulfonyl)imide ([EVIM][Tf<sub>2</sub>N],  $\geq$ 99%) were purchased from (NaOH), methanol (MeOH), ethanol (EtOH), acetonitrile (MeCN), *N,N*-dimethylformamide (DMF), tetrahydrofuran (THF), ethyl acetate, methylbenzene, heptane, silver nitrate (AgNO<sub>3</sub>), and anhydrous ferric chloride (FeCl<sub>3</sub>) were purchased from Sinopharm Chemical Reagent Co., Ltd. (China). The deionized water was gotten from the Wahaha Group Co., Ltd (China). The mixtures of tocopherols (88.6 wt%), containing 18.0 wt%  $\delta$ -tocopherol, 57.6 wt%  $\beta$ - and  $\gamma$ -tocopherol, and 13.0 wt%  $\alpha$ -tocopherol, were obtained from Zhejiang Worldbestve Biotechnology Co., Ltd. (China). Activated carbon was purchased from Shaowu Xinsen Charcoal Industry Co., Ltd. (Fujian, China). Methanol used in HPLC analysis was guaranteed reagents (GR) and were achieved from TEDIA (USA). Carbon dioxide (CO<sub>2</sub>, gas, 99.995%), nitrogen (N<sub>2</sub>, gas, 99.999%), acetylene (C<sub>2</sub>H<sub>2</sub>, gas, 99.0%) and ethylene (C<sub>2</sub>H<sub>4</sub>, gas, 99.99%) were gotten from Hangzhou Jingong Special Gas Co., Ltd. (China).

Notably, Amberlite XAD-4 resin was successively washed by ethanol, aqueous HCl standard solution, deionized water, aqueous NaOH solution (NaOH, 4 wt%) and deionized water; Amberlite 717 resin was immersed in aqueous HCl standard solution over night and washed by deionized water; activated carbon was wash by deionized water under ultrasonic conditions. After above procedures, these materials were filtered and dried at room temperature with reduced pressure.

## Characterization

N<sub>2</sub> sorption experiments were performed with a TriStar II Plus 2.02 (Micromeritics Corp., USA) at liquid nitrogen temperature (77K). The surface area was evaluated from N<sub>2</sub> adsorption isotherm in the relative pressure ( $P/P_0$ ) from 0.05 to 0.30 using the Brunauer-Emmett-Teller (BET) equation, the total pore volume was determined at  $P/P_0 = 0.990$ , the pore size distribution for mesopores and mesopore volume were calculated using the Barrett-Joyner-Halenda (BJH) model, as well as the external surface area, micropore surface area and micropore volume were estimated by the t-plot method. All samples were degassed at 100 °C for 12 h prior to the measurements.

Elemental analysis (EA) was carried out for carbon, hydrogen and nitrogen using a Vario Micro cube Elemental Analyzer (Elementar Corp., Germany).

Fourier transform infrared spectroscopy (FTIR) spectra were recorded under ambient conditions in the wave number range of 4000-525 cm<sup>-1</sup> using a Nicolet 6700 FTIR instrument; samples were measured in solid state with a single reflection diamond ATR.

Thermogravimetric analysis (TGA) measurements were implemented on a Q500 TGA (TA Corp., USA), over the temperature range from 50 to 800 °C under N<sub>2</sub> at a heating rate of 10 °C min<sup>-1</sup>.

Polymer morphology was investigated with a SIRION-100 field emission scanning electron microscopy (SEM) machine (FEI Corp., USA) at 3 KV, samples were previously sputter-coated with Au before imaging. Transmission electron microscopy (TEM) images were obtained using a HT7700 electron microscopy (Hitachi Corp., Japan) working at 100 kV.

Nuclear magnetic resonance (NMR) spectra were recorded with an AVANCE III model 400 MHz spectrometer (Bruker Corp. Germany) using TMS as internal reference at room temperature, and DMSO-*d*<sub>6</sub> and chloroform (CDCl<sub>3</sub>) were utilized as solvents.

Adsorbates (tocopherol homologues and organic phenolic compounds) were detected by HPLC system (Waters Corp., USA) including Waters 1525 binary pump, 2487 dual  $\lambda$  absorbance detector and 717 plus autosampler, as well as a Atiantis T3 column (5  $\mu$ m, 4.6 $\times$ 250 mm); in the case of tocopherol homologues, a mixture of MeOH and H<sub>2</sub>O (95/5, v/v) was served as mobile phase with the column temperature of 40 °C, flow rate of 1 ml min<sup>-1</sup> and detection wavelength of 292 nm; in the case of organic phenolic compounds, a mixture of MeOH and H<sub>2</sub>O (70/30, v/v) was used as mobile phase with the column temperature of 30 °C, flow rate of 0.5 ml min<sup>-1</sup> and detection wavelength of 272 nm.

## The characterization of [EVIM][Br] and long-chain carboxylate ionic liquids (LCC-ILs)

**1-ethyl-3-vinylimidazolium bromide ([EVIM][Br])** :  $^1\text{H}$  NMR  $\delta_H$  (400 MHz, DMSO- $d_6$ , ppm) 9.77 (1H, s, -N-CH-N-), 8.31 (1H, s, -N-CHCH-N-), 8.05 (1H, s, -N-CHCH-N-), 7.37 (1H, dd, -CH=CH<sub>2</sub>), 6.05 (1H, dd, -CH=CH<sub>2</sub>), 5.44 (1H, dd, -CH=CH<sub>2</sub>), 4.28 (2H, q, -N-CH<sub>2</sub>-CH<sub>3</sub>), 1.47 (3H, t, -N-CH<sub>2</sub>-CH<sub>3</sub>).  $^{13}\text{C}$  NMR  $\delta_C$  (100 MHz, DMSO- $d_6$ , ppm) 135.06, 128.80, 122.94, 119.10, 108.53, 44.56, 14.78.

**1-ethyl-3-vinylimidazolium acetate ([EVIM][C<sub>1</sub>COO])** :  $^1\text{H}$  NMR  $\delta_H$  (400 MHz, DMSO- $d_6$ , ppm) 9.98 (1H, s, -N-CH-N-), 8.22 (1H, s, -N-CHCH-N-), 7.96 (1H, s, -N-CHCH-N-), 7.36 (1H, dd, -CH=CH<sub>2</sub>), 5.99 (1H, dd, -CH=CH<sub>2</sub>), 5.40 (1H, dd, -CH=CH<sub>2</sub>), 4.28 (2H, q, -N-CH<sub>2</sub>-CH<sub>3</sub>), 1.62 (3H, s, CH<sub>3</sub>-COO), 1.39 (3H, t, -N-CH<sub>2</sub>-CH<sub>3</sub>).  $^{13}\text{C}$  NMR  $\delta_C$  (100 MHz, DMSO- $d_6$ , ppm) 173.70, 135.94, 129.00, 122.87, 119.01, 108.19, 44.44, 24.66, 14.77.

**1-ethyl-3-vinylimidazolium butyrate ([EVIM][C<sub>3</sub>COO])** :  $^1\text{H}$  NMR  $\delta_H$  (400 MHz, DMSO- $d_6$ , ppm) 10.02 (1H, s, -N-CH-N-), 8.23 (1H, s, -N-CHCH-N-), 7.96 (1H, s, -N-CHCH-N-), 7.38 (1H, dd, -CH=CH<sub>2</sub>), 6.00 (1H, dd, -CH=CH<sub>2</sub>), 5.39 (1H, dd, -CH=CH<sub>2</sub>), 4.25 (2H, q, -N-CH<sub>2</sub>-CH<sub>3</sub>), 1.89 (2H, t, -CH<sub>2</sub>-COO), 1.50-1.05 (5H, m, -N-CH<sub>2</sub>-CH<sub>3</sub> and -CH<sub>2</sub>-CH<sub>2</sub>-COO), 0.82 (3H, t, CH<sub>3</sub>-CH<sub>2</sub>-CH<sub>2</sub>-COO).  $^{13}\text{C}$  NMR  $\delta_C$  (100 MHz, DMSO- $d_6$ , ppm) 175.94, 135.78, 128.98, 122.88, 119.00, 108.24, 44.47, 39.15, 19.15, 14.76, 14.15.

**1-ethyl-3-vinylimidazolium hexanoate ([EVIM][C<sub>5</sub>COO])** :  $^1\text{H}$  NMR  $\delta_H$  (400 MHz, DMSO- $d_6$ , ppm) 9.85 (1H, s, -N-CH-N-), 8.22 (1H, s, -N-CHCH-N-), 7.94 (1H, s, -N-CHCH-N-), 7.33 (1H, dd, -CH=CH<sub>2</sub>), 5.98 (1H, dd, -CH=CH<sub>2</sub>), 5.40 (1H, dd, -CH=CH<sub>2</sub>), 4.24 (2H, q, -N-CH<sub>2</sub>-CH<sub>3</sub>), 1.94 (2H, t, -CH<sub>2</sub>-COO), 1.50-1.05 (9H, m, -N-CH<sub>2</sub>-CH<sub>3</sub> and -(CH<sub>2</sub>)<sub>3</sub>-CH<sub>2</sub>-COO), 0.84 (3H, t, CH<sub>3</sub>-(CH<sub>2</sub>)<sub>3</sub>-CH<sub>2</sub>-COO).  $^{13}\text{C}$  NMR  $\delta_C$  (100 MHz, DMSO- $d_6$ , ppm) 176.07, 135.69, 128.95, 122.90, 119.02, 108.23, 44.48, 36.70, 31.37, 25.45, 22.03, 14.76, 13.90.

**1-ethyl-3-vinylimidazolium octoate ([EVIM][C<sub>7</sub>COO])** :  $^1\text{H}$  NMR  $\delta_H$  (400 MHz, DMSO- $d_6$ , ppm) 9.81 (1H, s, -N-CH-N-), 8.21 (1H, s, -N-CHCH-N-), 7.95 (1H, s, -N-CHCH-N-), 7.34 (1H, dd, -CH=CH<sub>2</sub>), 5.98 (1H, dd, -CH=CH<sub>2</sub>), 5.40 (1H, dd, -CH=CH<sub>2</sub>), 4.24 (2H, q, -N-CH<sub>2</sub>-CH<sub>3</sub>), 1.95 (2H, t, -CH<sub>2</sub>-COO), 1.50-1.05 (13H, m, -N-CH<sub>2</sub>-CH<sub>3</sub> and -(CH<sub>2</sub>)<sub>5</sub>-CH<sub>2</sub>-COO), 0.85 (3H, t, CH<sub>3</sub>-(CH<sub>2</sub>)<sub>5</sub>-CH<sub>2</sub>-COO).  $^{13}\text{C}$  NMR  $\delta_C$  (100 MHz, DMSO- $d_6$ , ppm) 176.00, 136.06, 129.03, 122.86, 118.99, 108.12, 44.43, 37.55, 31.33, 29.25, 28.74, 26.13, 22.10, 14.79, 13.92.

**1-ethyl-3-vinylimidazolium decanoate ([EVIM][C<sub>9</sub>COO])** :  $^1\text{H}$  NMR  $\delta_H$  (400 MHz, DMSO- $d_6$ , ppm) 9.91 (1H, s, -N-CH-N-), 8.22 (1H, s, -N-CHCH-N-), 7.95 (1H, s, -N-CHCH-N-), 7.36 (1H, dd, -CH=CH<sub>2</sub>), 5.98 (1H, dd, -CH=CH<sub>2</sub>), 5.40 (1H, dd, -CH=CH<sub>2</sub>), 4.24 (2H, q, -N-CH<sub>2</sub>-CH<sub>3</sub>), 1.94 (2H, t, -CH<sub>2</sub>-COO), 1.50-1.05 (17H, m, -N-CH<sub>2</sub>-CH<sub>3</sub> and -(CH<sub>2</sub>)<sub>7</sub>-CH<sub>2</sub>-COO), 0.85 (3H, t, CH<sub>3</sub>-(CH<sub>2</sub>)<sub>7</sub>-CH<sub>2</sub>-COO).  $^{13}\text{C}$  NMR  $\delta_C$  (100 MHz, DMSO- $d_6$ , ppm) 175.80, 135.69, 128.96, 122.89, 119.00, 108.25, 44.48, 36.70, 31.30, 29.13, 29.02, 28.72, 25.77, 22.08, 14.76, 13.91.

**1-ethyl-3-vinylimidazolium laurate ([EVIM][C<sub>11</sub>COO])** :  $^1\text{H}$  NMR  $\delta_H$  (400 MHz, DMSO- $d_6$ , ppm) 9.95 (1H, s, -N-CH-N-), 8.22 (1H, s, -N-CHCH-N-), 7.95 (1H, s, -N-CHCH-N-), 7.36 (1H, dd, -CH=CH<sub>2</sub>), 5.98 (1H, dd, -CH=CH<sub>2</sub>), 5.40 (1H, dd, -CH=CH<sub>2</sub>), 4.23 (2H, q, -N-CH<sub>2</sub>-CH<sub>3</sub>), 1.90 (2H, t, -CH<sub>2</sub>-COO), 1.50-1.05 (21H, m, -N-CH<sub>2</sub>-CH<sub>3</sub> and -(CH<sub>2</sub>)<sub>9</sub>-CH<sub>2</sub>-COO), 0.85 (3H, t, CH<sub>3</sub>-(CH<sub>2</sub>)<sub>9</sub>-CH<sub>2</sub>-COO).  $^{13}\text{C}$  NMR  $\delta_C$  (100 MHz, DMSO- $d_6$ , ppm) 176.04, 136.26, 129.06, 122.86, 119.00, 107.99, 44.39, 37.68, 31.30, 29.31, 29.11, 29.05, 28.73, 26.17, 22.08, 14.82, 13.88.

**1-ethyl-3-vinylimidazolium myristate ([EVIM][C<sub>13</sub>COO])** :  $^1\text{H}$  NMR  $\delta_H$  (400 MHz, CDCl<sub>3</sub>, ppm) 11.30 (1H, s, -N-CH-N-), 7.63 (1H, s, -N-CHCH-N-), 7.52 (1H, dd, -CH=CH<sub>2</sub>), 7.38 (1H, s, -N-CHCH-N-), 5.77 (1H, dd, -CH=CH<sub>2</sub>), 5.33 (1H, dd, -CH=CH<sub>2</sub>), 4.39 (2H, q, -N-CH<sub>2</sub>-CH<sub>3</sub>), 2.23 (2H, t, -CH<sub>2</sub>-COO), 1.68-1.00 (25H, m, -N-CH<sub>2</sub>-CH<sub>3</sub> and -(CH<sub>2</sub>)<sub>11</sub>-CH<sub>2</sub>-COO), 0.88 (3H, t, CH<sub>3</sub>-(CH<sub>2</sub>)<sub>11</sub>-CH<sub>2</sub>-COO).  $^{13}\text{C}$  NMR  $\delta_C$  (100 MHz, CDCl<sub>3</sub>, ppm) 179.52, 138.71, 129.00, 121.58, 118.07, 108.44, 45.37, 37.19, 31.91, 29.71, 29.65, 29.58, 29.36, 26.26, 22.68, 15.38, 14.12.

**1-ethyl-3-vinylimidazolium palmitate ([EVIM][C<sub>15</sub>COO])** :  $^1\text{H}$  NMR  $\delta_H$  (400 MHz, CDCl<sub>3</sub>, ppm) 11.32 (1H, s, -N-CH-N-), 7.67 (1H, s, -N-CHCH-N-), 7.51 (1H, dd, -CH=CH<sub>2</sub>), 7.41 (1H, s, -N-CHCH-N-), 5.82 (1H, dd, -CH=CH<sub>2</sub>), 5.34 (1H, dd, -CH=CH<sub>2</sub>), 4.40 (2H, q, -N-CH<sub>2</sub>-CH<sub>3</sub>), 2.23 (2H, t, -CH<sub>2</sub>-COO), 1.68-1.00 (29H, m, -N-CH<sub>2</sub>-CH<sub>3</sub> and -(CH<sub>2</sub>)<sub>13</sub>-CH<sub>2</sub>-COO), 0.88 (3H, t, CH<sub>3</sub>-(CH<sub>2</sub>)<sub>13</sub>-CH<sub>2</sub>-COO).  $^{13}\text{C}$  NMR  $\delta_C$  (100 MHz, CDCl<sub>3</sub>, ppm) 179.59, 138.45, 128.92, 121.70, 118.23, 108.59, 45.39, 37.33, 31.91, 29.71, 29.65, 29.59, 29.35, 26.32, 22.68, 15.41, 14.12.

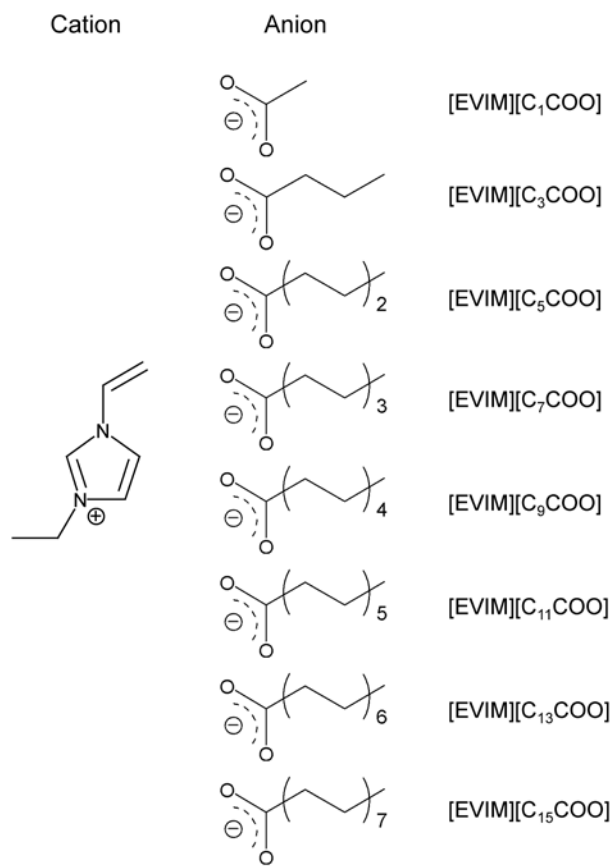


**Fig. S1** Molecular structures of LCC-ILs

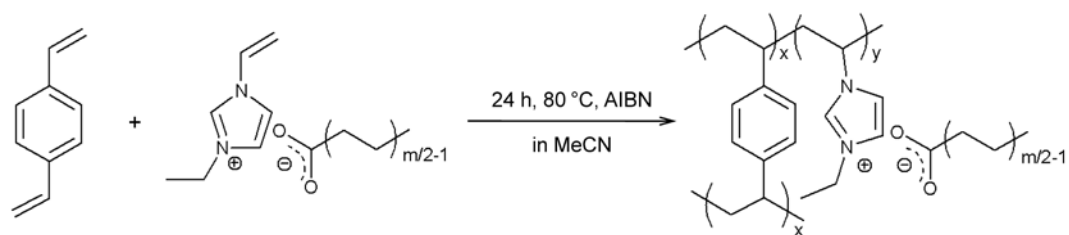


**Fig. S2** Synthetic route of P(nDVB-EVIMCm)s using LCC-ILs, n represents the used molar ratio of DVB to LCC-ILs, m represents the even carbon number of the carboxylate anions and changes from 2 to 16.

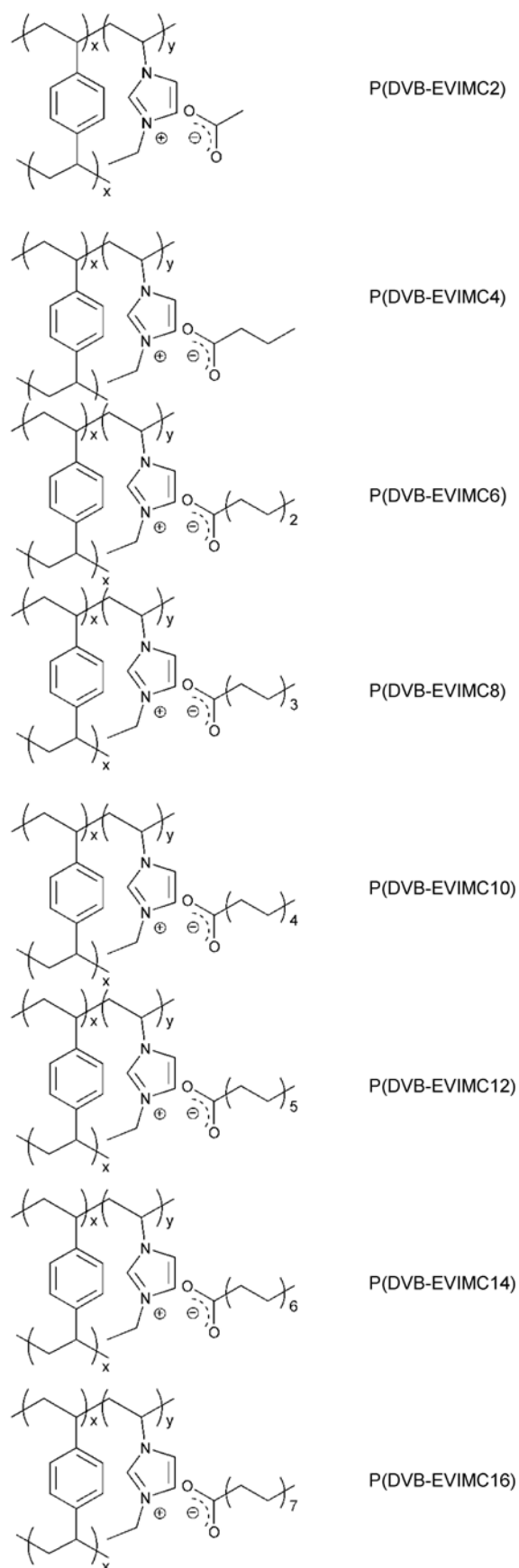


**Fig. S3** Molecular structures of P(DVB-EVIMCm)s using LCC-ILs .

**Table S1** Solvent selection and textural parameters of P(DVB-EVIMC12)<sup>a</sup>

Entry	Solvent	$S_{\text{BET}}^b$ $\text{m}^2 \text{g}^{-1}$	$S_{\text{micro}}^c$ $\text{m}^2 \text{g}^{-1}$	$V_{\text{total}}^d$ $\text{cm}^3 \text{g}^{-1}$	$V_{\text{micro}}^e$ $\text{cm}^3 \text{g}^{-1}$	$D_{\text{BJH}}^f$ nm	IL content <sup>g</sup> $\text{mmol g}^{-1}$
1	EtOH	172	24	0.386	0.003	10.4	0.83
2	MeOH	203	42	0.326	0.017	8.4	0.74
3	H <sub>2</sub> O/MeCN=0.1 <sup>h</sup>	241	11	0.318	0.011	7.4	0.79
4	H <sub>2</sub> O/MeCN=0.2 <sup>h</sup>	174	5	0.211	0.011	6.4	0.62
5	others <sup>i</sup>	n.d. <sup>j</sup>	n.d.	n.d.	n.d.	n.d.	0.99-1.32

<sup>a</sup> Polymers synthesized with equimolar DVB and [EVIM][C<sub>11</sub>COO], 2 wt% AIBN at 80 °C for 24 h. <sup>b</sup> BET surface area evaluated from N<sub>2</sub> adsorption isotherm in the relative pressure(P/P<sub>0</sub>) from 0.05 to 0.30. <sup>c</sup> Micropore surface area calculated from *t*-plot method. <sup>d</sup> Total pore volume at P/P<sub>0</sub> = 0.990. <sup>e</sup> Micropore volume derived from *t*-plot method. <sup>f</sup> Average mesopore size calculated from BJH model. <sup>g</sup> Loading of ILs on the polymer and determined from the elemental analysis. <sup>h</sup> H<sub>2</sub>O/MeCN volume ratio of 0.1 and 0.2, respectively. <sup>i</sup> Others are DMF, acetone, ethyl acetate, THF and methyl benzene. <sup>j</sup> Not determined.

**Table S2** Textural parameters of P(nDVB-EVIMC12)s<sup>a</sup>

Entry	Sample	$S_{\text{BET}}$ $\text{m}^2 \text{g}^{-1}$	$S_{\text{micro}}$ $\text{m}^2 \text{g}^{-1}$	$V_{\text{total}}$ $\text{cm}^3 \text{g}^{-1}$	$V_{\text{micro}}$ $\text{cm}^3 \text{g}^{-1}$	$D_{\text{BJH}}$ nm	IL content $\text{mmol g}^{-1}$
1	P(0.5DVB-EVIMC12)	2.	n.d.	0.003	n.d.	n.d.	1.75
2	P(0.75DVB-EVIMC12)	194	4	0.520	0.006	16.0	1.32
3	P(2DVB-EVIMC12)	279	59	0.187	0.036	2.9	0.66
4	P(3DVB-EVIMC12)	349	123	0.216	0.072	2.7	0.53
5	P(5DVB-EVIMC12)	393	109	0.249	0.075	3.0	0.31

<sup>a</sup> n stands for the molar ratio of DVB to [EVIM][C<sub>11</sub>COO].

**Table S3** Several other reaction conditions and textural parameters of P(DVB-EVIMC12)

Entry	T °C	t h	AIBN wt% <sup>a</sup>	$S_{\text{BET}}$ $\text{m}^2 \text{g}^{-1}$	$S_{\text{micro}}$ $\text{m}^2 \text{g}^{-1}$	$V_{\text{total}}$ $\text{cm}^3 \text{g}^{-1}$	$V_{\text{micro}}$ $\text{cm}^3 \text{g}^{-1}$	$D_{\text{BJH}}$ nm	IL content $\text{mmol g}^{-1}$
1	60	24	2	31	n.d.	0.028	0.007	4.0	0.78
2	100	24	2	132	12	0.237	0.013	6.7	1.10
3	80	3	2	5	n.d.	0.013	0.001	n.d.	0.69
4	80	6	2	43	8	0.044	0.010	4.8	1.16
5	80	12	2	235	37	0.436	0.018	9.3	1.04
6	80	24	1	25	n.d.	0.026	n.d.	5.2	0.82
7	80	24	3	264	17	0.375	0.014	7.4	1.21
8	80	24	4	130	n.d.	0.436	0.011	13.0	1.23

<sup>a</sup> The mass fraction of the total mass of DVB and the used ILs.

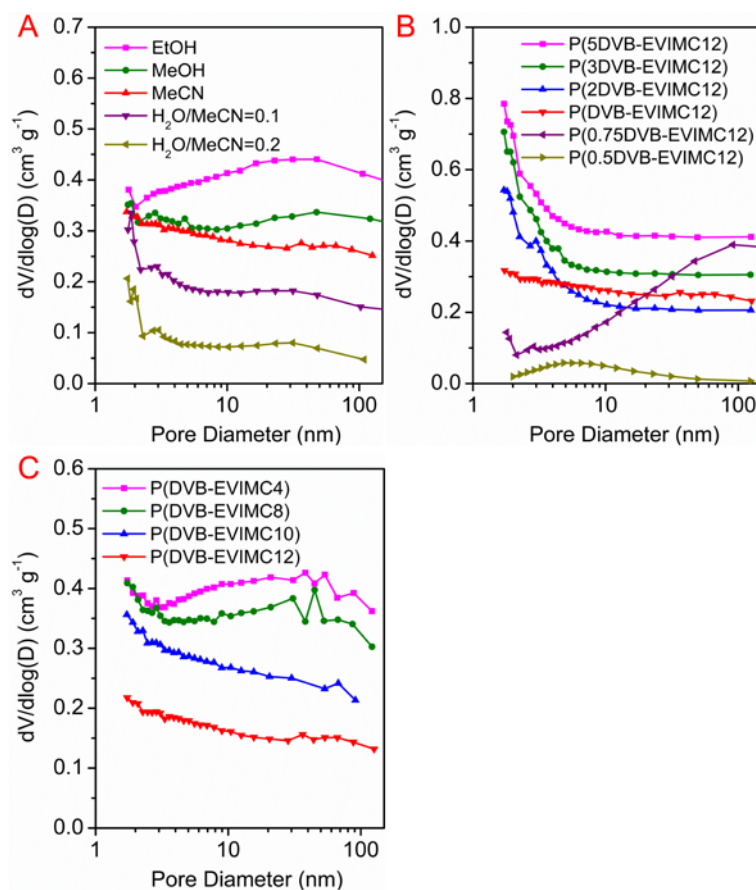
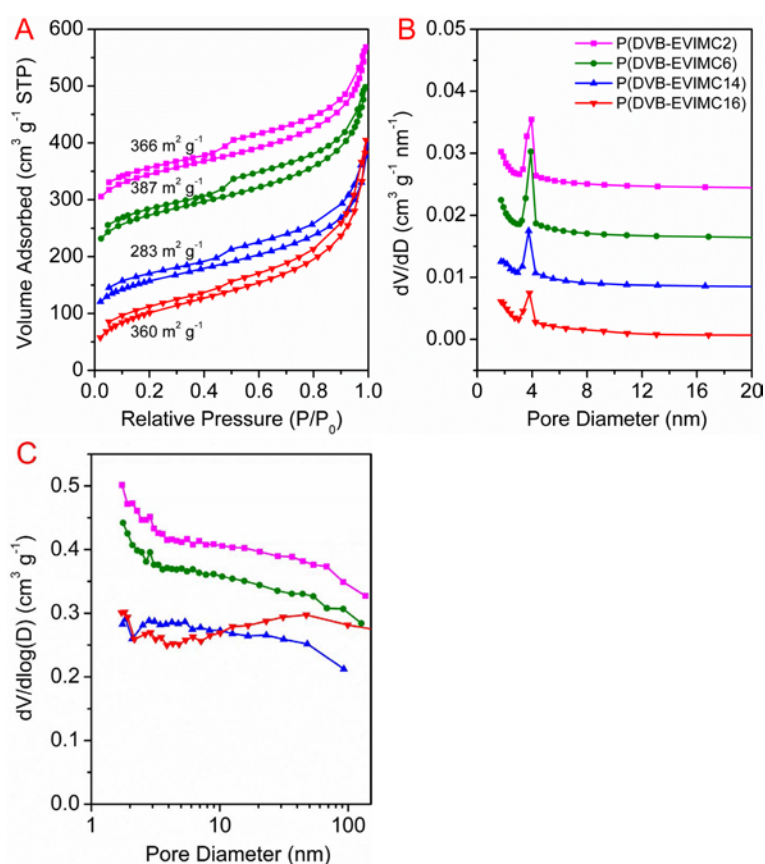


**Fig. S4** Pore size distributions of prepared polymers, and each of them was estimated by BJH model from an adsorption branch of  $\text{N}_2$  adsorption/desorption isotherm. (A) P(DVB-EVIMC12) synthesized in various solvents, the pore size distributions were shifted by 0, 0.06, 0.12, 0.18, and  $0.24 \text{ cm}^3 \text{g}^{-1}$  from the bottom up, respectively. (B) P(nDVB-EVIMC12)s, the ordinate values of the pore size distributions were shifted by 0, 0.1, 0.2, 0.3 and  $0.4 \text{ cm}^3 \text{g}^{-1}$ , respectively, except for P(0.75DVB-EVIMC12). (C) P(DVB-EVIMCm)s, the ordinate values of the pore size distributions were shifted by 0, 0.06, 0.12 and  $0.18 \text{ cm}^3 \text{g}^{-1}$ , respectively.

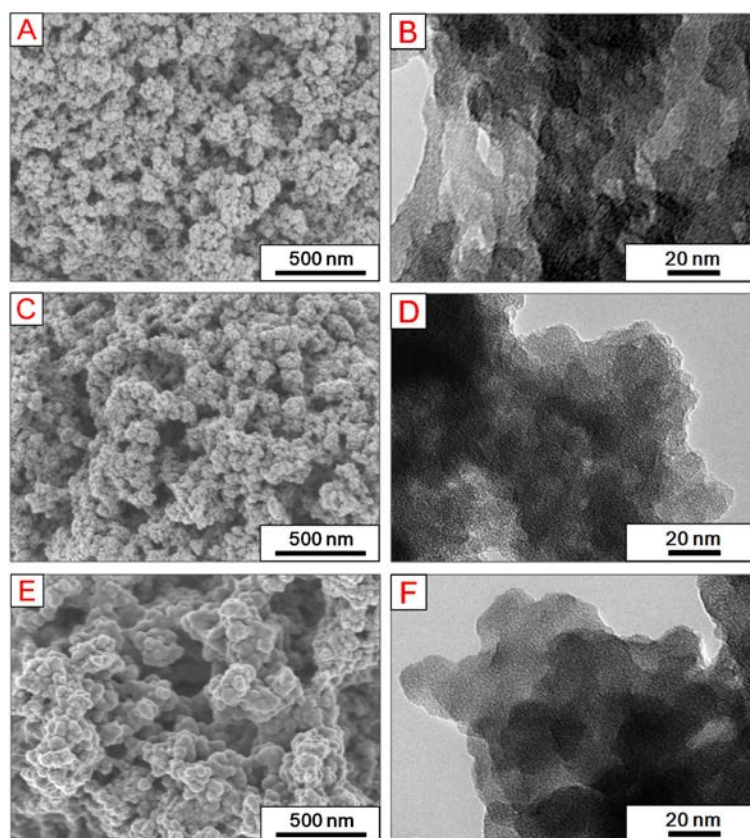
**Table S4** Textural parameters of several P(DVB-EVIMCm)s<sup>a</sup>

Entry	Sample	Solvent	$S_{\text{BET}}$ $\text{m}^2 \text{g}^{-1}$	$S_{\text{micro}}$ $\text{m}^2 \text{g}^{-1}$	$V_{\text{total}}$ $\text{cm}^3 \text{g}^{-1}$	$V_{\text{micro}}$ $\text{cm}^3 \text{g}^{-1}$	$D_{\text{BJH}}$ nm	IL content $\text{mmol g}^{-1}$
1	P(DVB-EVIMC2)	MeCN	366	31	0.508	0.015	6.8	1.04
2	P(DVB-EVIMC6)	MeCN	387	42	0.523	0.024	6.9	1.05
3	P(DVB-EVIMC14)	MeCN	144	n.d.	0.129	n.d.	4.1	0.99
4	P(DVB-EVIMC14)	EtOH	283	33	0.482	0.013	7.7	0.78
5	P(DVB-EVIMC16)	MeCN	1	0.1	0.001	0.001	1.7	2.58
6	P(DVB-EVIMC16)	EtOH	360	40	0.620	0.012	8.4	0.83

<sup>a</sup> Polymers synthesized with equimolar DVB and [EVIM][C<sub>11</sub>COO], 2 wt% AIBN at 80 °C for 24 h.



**Fig.S5** (A)  $\text{N}_2$  adsorption/desorption isotherms of P(DVB-EVIMC2), P(DVB-EVIMC6) synthesized in MeCN and P(DVB-EVIMC14), P(DVB-EVIMC14) synthesized in EtOH, the the ordinate values of the isotherms were shifted by 0, 80, 160 and 240  $\text{cm}^3 \text{g}^{-1}$  from the bottom up, respectively. (B) The ordinate values of the pore size distributions which were estimated by BJH model from the corresponding desorption branch of the isotherm, were shifted by 0, 0.008, 0.016 and 0.024  $\text{cm}^3 \text{g}^{-1} \text{nm}^{-1}$  from the bottom up, respectively. (C) The ordinate values of the pore size distributions which were estimated by BJH model from the corresponding adsorption branch of the isotherm, were shifted by 0, 0.1, 0.2 and 0.3  $\text{cm}^3 \text{g}^{-1}$ , respectively.

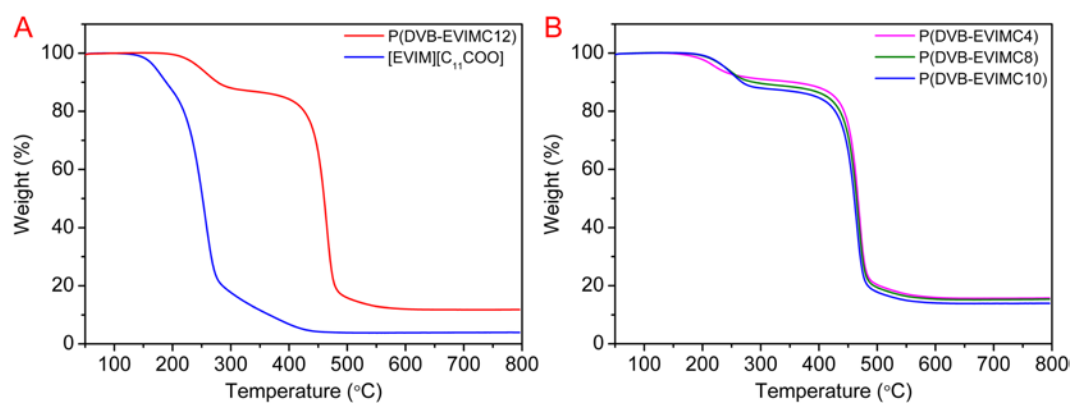


**Fig. S6** (A, C, E) SEM micrographs and (B, D, F) TEM images of P(DVB-EVIMC4), P(DVB-EVIMC8), P(DVB-EVIMC10).

**Table S5** Thermogravimetric results of representative P(DVB-EVIMCm)s and LCC-ILs

Entry	Sample	Weight loss	T <sub>onset</sub> <sup>a</sup> (°C)
1	[EVIM][C <sub>3</sub> COO]	8.51	161
2	P(DVB-EVIMC4)	1.11	184
3	[EVIM][C <sub>7</sub> COO]	13.92	198
4	P(DVB-EVIMC8)	1.23	206
5	[EVIM][C <sub>9</sub> COO]	14.19	202
6	P(DVB-EVIMC10)	1.47	211
7	[EVIM][C <sub>11</sub> COO]	18.50	216
8	P(DVB-EVIMC12)	1.53	220

<sup>a</sup>T<sub>onset</sub> stands for onset temperature of decomposition.

**Fig. S7** Thermogravimetric curves of representative P(DVB-EVIMCm)s and LCC-ILs under nitrogen.

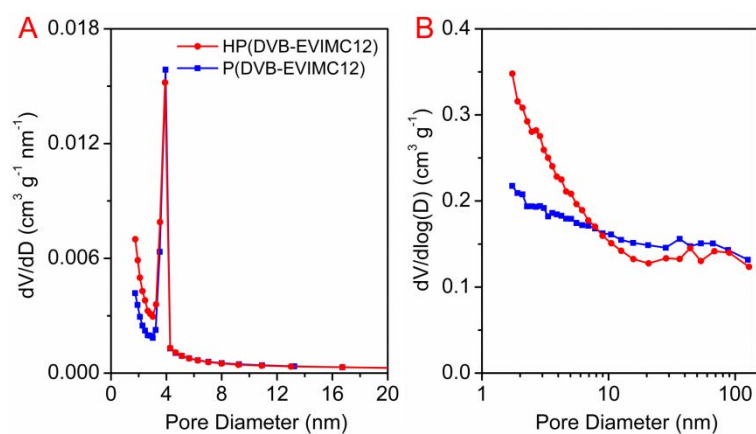


**Fig. S8** Pore size distributions of HP(DVB-EVIMC12) and P(DVB-EVIMC12). (A) Each of them was estimated by BJH model from an adsorption branch of  $\text{N}_2$  adsorption/desorption isotherm. (B) Each of them was estimated by BJH model from a desorption branch.

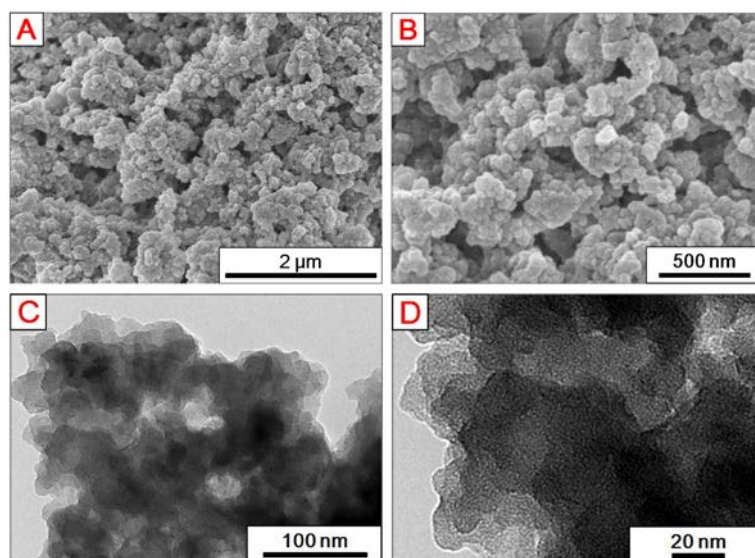


**Fig. S9** (A) and (B) SEM micrographs of HP(DVB-EVIMC12), (C) and (D) TEM images of HP(DVB-EVIMC12).

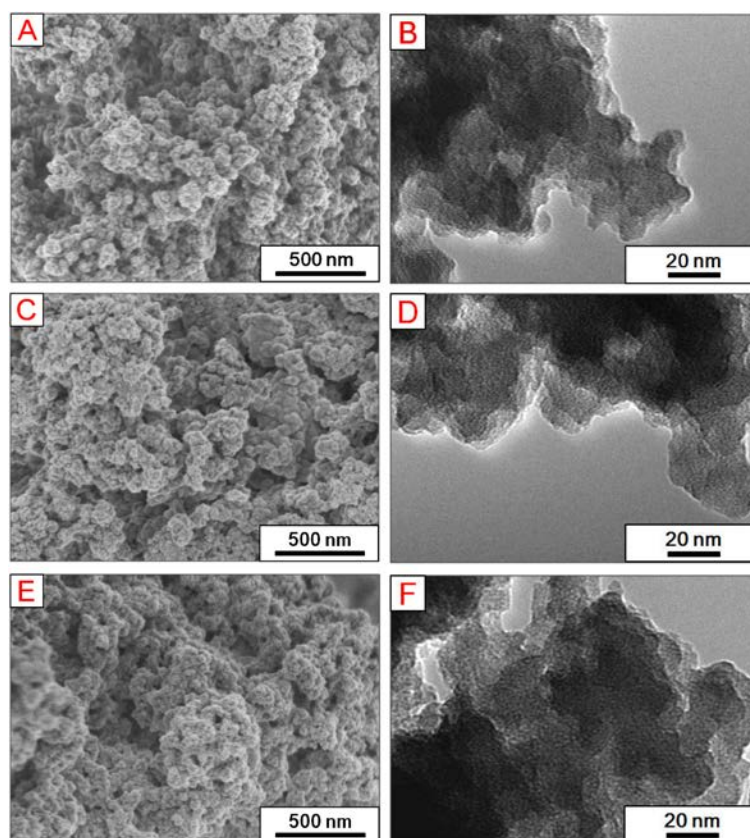


**Fig. S10** (A, C, E) SEM micrographs and (B, D, F) TEM images of HP(DVB-EVIMC4), HP(DVB-EVIMC8), HP(DVB-EVIMC10).

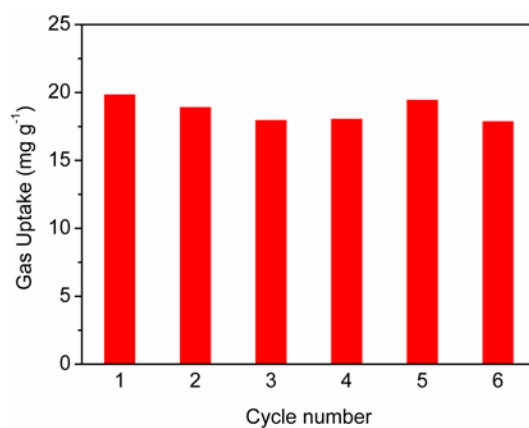


**Fig. S11** Six cycles of CO<sub>2</sub> uptake on P(DVB-EVIMC10) at 25 °C. After adsorption, the sample was regenerated at 100 °C for 6 h

**Table S6** Dual-site Langmuir-Freundlich parameters for CO<sub>2</sub> and N<sub>2</sub> isotherms of P(DVB-EVIMCm)s and HP(DVB-EVIMCm)s at 25 or 0 °C.

Sample	Gas	T °C	Site A			Site B			R <sup>2</sup>
			$q_{A,sat}$ mol kg <sup>-1</sup>	$b_A$ kPa <sup>-v<sub>i</sub></sup>	$v_A$ dimensionless	$q_{B,sat}$ mol kg <sup>-1</sup>	$b_B$ kPa <sup>-v<sub>i</sub></sup>	$v_B$ dimensionless	
P(DVB-EVIMC4)	CO <sub>2</sub>	25	0.0312	0.6028	0.6055	3.7267	$1.568 \times 10^{-3}$	0.9591	1
	N <sub>2</sub>	25	0.1926	$7.822 \times 10^{-5}$	1.6684	$9.921 \times 10^{-5}$	2.3130	4.4005	0.9993
HP(DVB-EVIMC4)	CO <sub>2</sub>	25	0.2038	0.0224	0.9182	3.7874	$1.073 \times 10^{-3}$	1.0184	1
	N <sub>2</sub>	25	0.2760	$2.501 \times 10^{-4}$	1.3540	$1.616 \times 10^{-3}$	$5.212 \times 10^{-11}$	6.3992	0.9997
P(DVB-EVIMC8)	CO <sub>2</sub>	25	0.0470	1.4573	0.6330	3.6048	$1.855 \times 10^{-3}$	0.9346	1
	N <sub>2</sub>	25	0.0658	$1.286 \times 10^{-4}$	1.8967	$3.473 \times 10^{-3}$	0.2775	0.5554	0.9992
HP(DVB-EVIMC8)	CO <sub>2</sub>	25	0.3085	0.0182	0.8890	3.0129	$1.164 \times 10^{-3}$	1.0336	1
	N <sub>2</sub>	25	0.1017	$3.521 \times 10^{-4}$	1.5680	$6.385 \times 10^{-4}$	0.5122	1.6554	0.9993
P(DVB-EVIMC10)	CO <sub>2</sub>	25	0.0444	1.8448	0.7491	3.5440	$1.804 \times 10^{-3}$	0.7491	1
	N <sub>2</sub>	25	1.8642	$4.041 \times 10^{-5}$	1.2944	$1.266 \times 10^{-3}$	$1.069 \times 10^{-11}$	7.0189	0.9997
HP(DVB-EVIMC10)	CO <sub>2</sub>	25	0.6115	0.0147	0.9815	0.8333	$1.115 \times 10^{-4}$	1.7494	1
	N <sub>2</sub>	25	0.1484	$4.190 \times 10^{-4}$	1.4060	$3.753 \times 10^{-4}$	4.0992	1.8549	0.9996
P(DVB-EVIMC12)	CO <sub>2</sub>	25	0.0277	0.5331	0.6891	4.7596	$9.307 \times 10^{-4}$	0.9973	1
	N <sub>2</sub>	25	0.0920	$2.620 \times 10^{-4}$	1.5820	$4.603 \times 10^{-4}$	0.4346	1.6901	0.9991
	CO <sub>2</sub>	0	0.2184	0.0580	0.6122	6.5938	$1.401 \times 10^{-3}$	0.8958	1
	N <sub>2</sub>	0	0.4597	$2.084 \times 10^{-4}$	1.3942	$6.155 \times 10^{-4}$	1.7346	1.7373	0.9998
HP(DVB-EVIMC12)	CO <sub>2</sub>	25	0.0596	0.0912	1.0728	1.8650	$1.323 \times 10^{-3}$	1.2141	1
	N <sub>2</sub>	25	0.0799	$7.916 \times 10^{-4}$	1.4783	$1.466 \times 10^{-3}$	2.5983	1.1428	0.9992
	CO <sub>2</sub>	0	0.1004	$2.419 \times 10^{-14}$	6.8227	1.8673	$9.218 \times 10^{-3}$	0.9043	1
	N <sub>2</sub>	0	0.1216	$1.379 \times 10^{-4}$	1.9414	$3.841 \times 10^{-3}$	$6.165 \times 10^{-3}$	2.6683	0.9991

**Table S7** Virial parameters for CO<sub>2</sub> adsorption isotherms of P(DVB-EVIMC12) and HP(DVB-EVIMC12) at 25 and 0 °C

Sample	a <sub>0</sub>	a <sub>1</sub>	a <sub>2</sub>	a <sub>3</sub>	a <sub>4</sub>	a <sub>5</sub>	b <sub>0</sub>	b <sub>1</sub>	b <sub>2</sub>	R <sup>2</sup>
P(DVB-EVIMC12)	-2479.8	99.944	-18.509	1.6153	-0.0545	$6.851 \times 10^{-4}$	10.615	0.1631	-0.0130	0.9980
HP(DVB-EVIMC12)	-2555.8	70.592	-1.9104	0.0799	-0.0020	$1.792 \times 10^{-4}$	11.637	-0.1801	0.0013	1

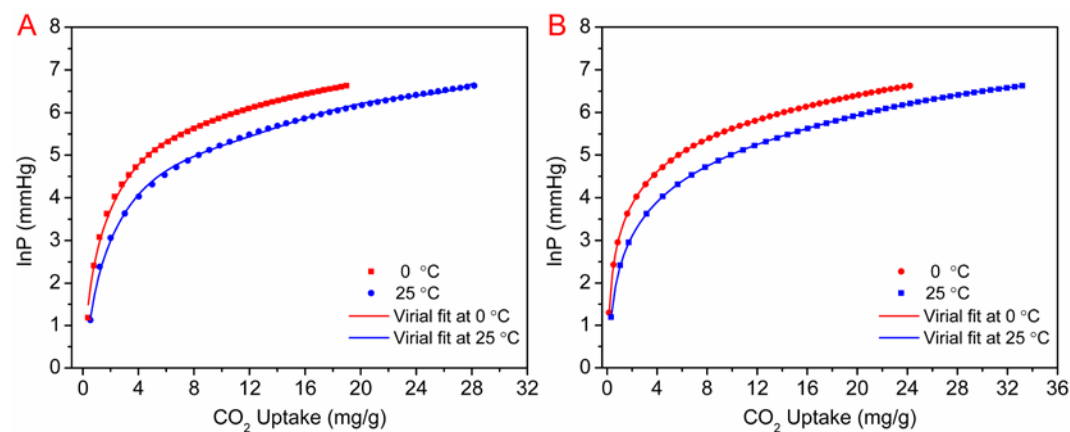


**Fig. S12** The fitting by Virial equation of CO<sub>2</sub> adsorption isotherms for (A) P(DVB-EVIMC12) and (B) HP(DVB-EVIMC12).

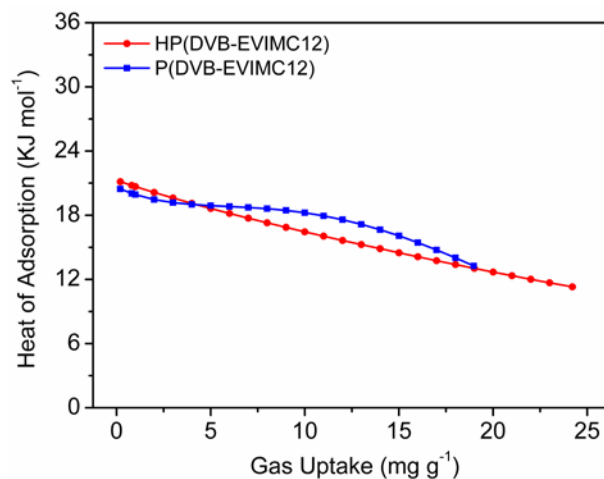


**Fig. S13** For P(DVB-EVIMC12) and HP(DVB-EVIMC12), isosteric heat of adsorption for CO<sub>2</sub> at different loadings, the adsorption isotherms fitted by Virial equation using the data at 25 and 0 °C.

**Table S8** Textural parameters of P(nDVB-IL)s with common ILs <sup>a</sup>

Entry	Sample <sup>b</sup>	Solvent	$S_{\text{BET}}$ $\text{m}^2 \text{g}^{-1}$	$S_{\text{micro}}$ $\text{m}^2 \text{g}^{-1}$	$V_{\text{total}}$ $\text{cm}^3 \text{g}^{-1}$	$V_{\text{micro}}$ $\text{cm}^3 \text{g}^{-1}$	$D_{\text{meso}}$ nm	IL content $\text{mmol g}^{-1}$
1	P(2DVB-EVIMBr)	mixture <sup>c</sup>	371	89	0.271	0.045	3.6	1.22
2	P(2DVB-EVIMBF <sub>4</sub> )	MeCN	374	67	0.446	0.031	6.4	1.06
3	P(2DVB-EVIMPF <sub>6</sub> )	MeCN	350	63	0.445	0.033	6.8	0.91
4	P(2DVB-EVIMTf <sub>2</sub> N)	MeCN	291	31	0.378	0.016	6.5	0.73

<sup>a</sup> n stands for the molar ratio of DVB to ILs. <sup>b</sup> Polymers synthesized with 2 wt% AIBN at 80 °C for 24 h. <sup>c</sup> P(2DVB-EVIMBr) obtained in the mixture of ethyl acetate, EtOH and H<sub>2</sub>O (volume ratio = 8:2:1).

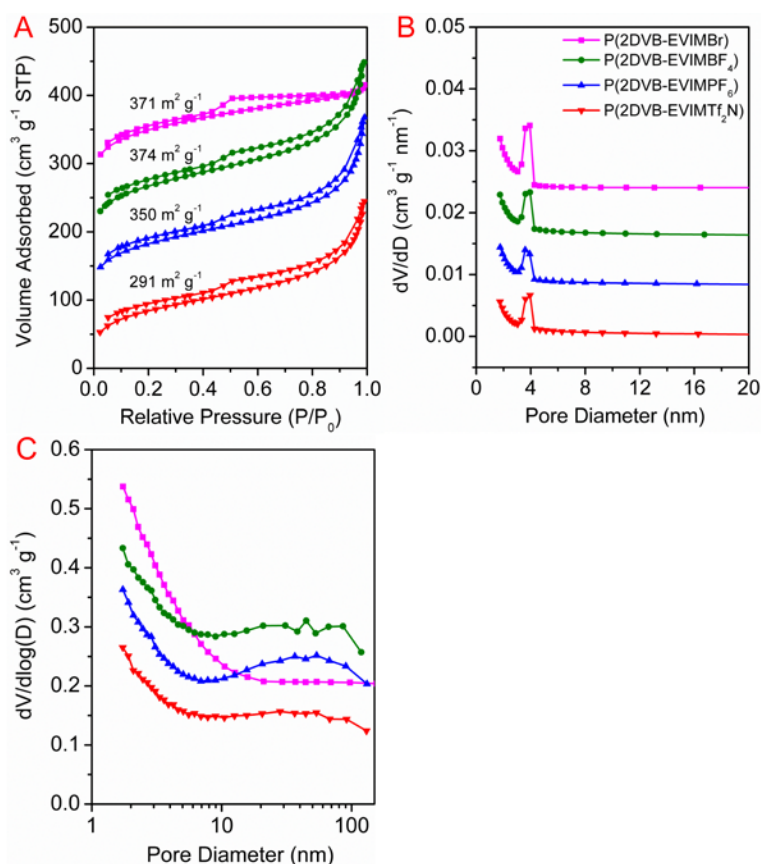


**Fig. S14** (A) N<sub>2</sub> adsorption/desorption isotherms of P(nDVB-IL)s with common ILs, the the ordinate values of the isotherms were shifted by 0, 80, 160 and 240 cm<sup>3</sup> g<sup>-1</sup> from the bottom up, respectively. (B) The ordinate values of pore size distributions which were estimated by BJH model from the corresponding desorption branch of the isotherm, were shifted by 0, 0.008, 0.016 and 0.024 cm<sup>3</sup> g<sup>-1</sup> nm<sup>-1</sup>, respectively. (C) The ordinate values of pore size distributions which were estimated by BJH model from the corresponding adsorption branch of the isotherm, were shifted by 0, 0.1, 0.2 and 0.3 cm<sup>3</sup> g<sup>-1</sup>, respectively.

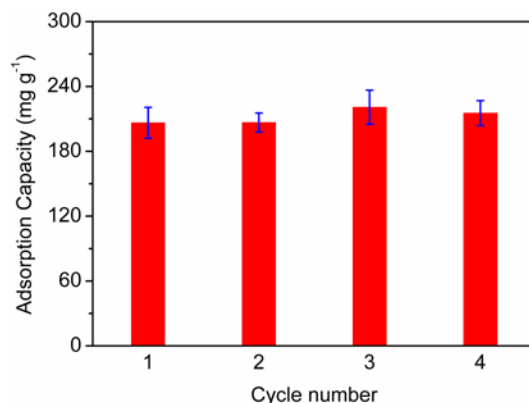


**Fig. S15** Four cycles of tocopherol adsorption on For P(DVB-EVIMC10) at 25 °C. After adsorption, regeneration was performed using ethanol as solvent at 45 °C for 8 h. All values are the mean of three measurements.

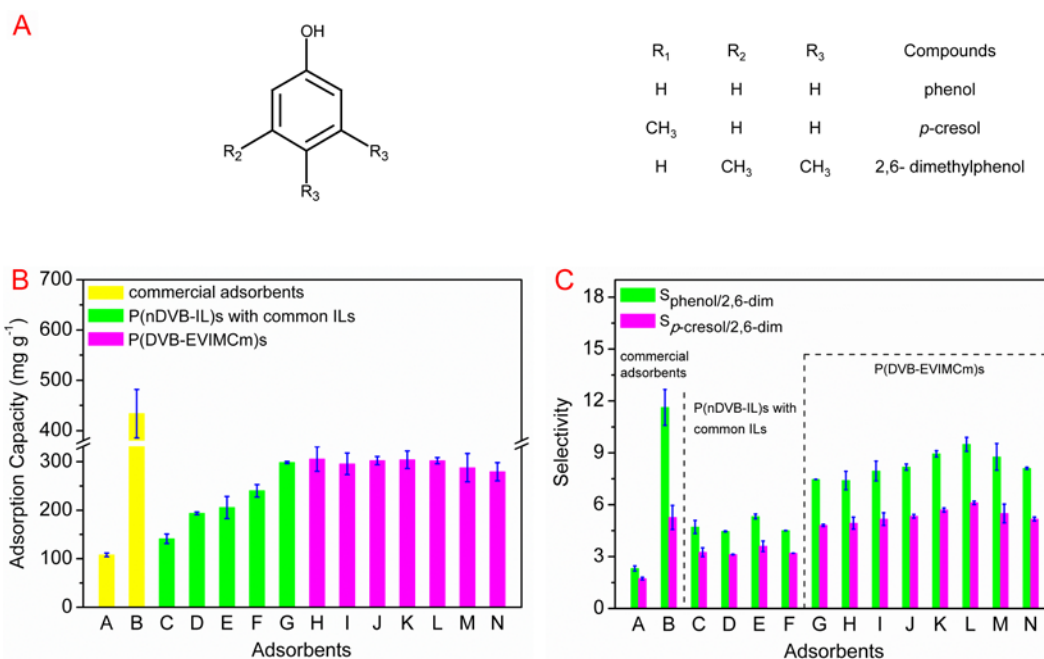


**Fig. S16** (A) Molecular structures of organic phenolic compounds. (B) Adsorption capacity and (C) selectivity of phenolic compounds in heptane by commercial adsorbents, P(nDVB-IL)s with common ILs and P(DVB-EVIMCm)s at 25 °C for 4 h. Adsorbents: A. Amberlite XAD-4 resin B. Amberlite 717 resin C. P(2DVB-EVIMTf<sub>2</sub>N) D. P(2DVB-EVIMPF<sub>6</sub>) E. P(2DVB-EVIMBr) F. P(2DVB-EVIMBF<sub>4</sub>) G. P(DVB-EVIMC2) H. P(DVB-EVIMC4) I. P(DVB-EVIMC6) J. P(DVB-EVIMC8) K. P(DVB-EVIMC10) L. P(DVB-EVIMC12) M. P(DVB-EVIMC14) N. P(DVB-EVIMC16). All values are the mean results of at least three measurements.